

**COB-2023-0058**

# VALIDATION OF AN ETHANOL-REDUCED CHEMICAL KINETIC MECHANISM AT SUPERCRITICAL CONDITIONS USING REAL GAS STATE EQUATION

**Paulo Vitor Ribeiro Plácido**  
**Rogério Gonçalves dos Santos**

School of Mechanical Engineering, University of Campinas UNICAMP, Rua Mendeleev, 200 - CEP 13083-860, Cidade Universitária "Zeferino Vaz", Barão Geraldo, Campinas/SP, Brazil  
vitorvrp@gmail.com, roger7@fem.unicamp.br

**Dario Alviso**

Laboratorio de Fluidodinámica, Facultad de Ingeniería, Universidad de Buenos Aires/CONICET, Paseo Colón 850, (1063) Buenos Aires, Argentina  
beto.alviso@gmail.com

## **Abstract.**

Several studies have been conducted to find an effective system to reduce particulate emissions from vehicle exhaust gas, which have become a primary source of air pollution in large cities. A promising system uses supercritical combustion, directly injecting fuel over its critical temperature and pressure. Supercritical fluids have a lower viscosity and surface tension than liquids and high diffusion rates, which promotes a uniform mixture distribution, improving thermal efficiency and reducing particulate emissions. This study focuses on supercritical Ethanol as a biofuel option to propose a reduced kinetic mechanism composed of 71 species and 684 reactions obtained by directed relation graph error propagation (DRGEP) and sensitivity analysis for simulating its combustion. This mechanism was validated using Cantera with a cubic Redlich-Kwong (RK) and an ideal (I) equation of state (EoS) through 0D constant-volume auto-ignition delay times (IDT) and an ideal EoS for laminar flame speed (LFS) simulations for pure Ethanol. The IDT results are consistent with experimental data at 10, 30, 50, 75, and 80 atm, in a temperature range of 700 - 1250 K, showing a satisfactory agreement with LFS experiments at 380 - 400 K, 1 - 4 atm and ( $\phi$ ) of 0.6 - 1.4.

**Keywords:** Chemical Kinetic Mechanism, Supercritical Combustion, Ethanol Mechanism, Ignition Delay Time, Redlich-Kwog.

## **1. INTRODUCTION**

In recent human history, vehicle logistics, and fossil fuel consumption has rapidly grown due to social development, especially in large metropolises. International attention has been focused on minimizing the impacts of air pollution and vehicle emissions on climate change and population health (Li *et al.*, 2016). Therefore, gas emission and fuel efficiency regulations require clean and highly efficient combustion systems. Improving internal combustion engines' fuel economy, combustion, and emission performance has been vital.

Although an elective technology system to improve the efficiency of gasoline engines is the direct injection of gasoline (GDI) Binder *et al.* (2015), it has a shorter time to mix fuel and air, this can lead to partial uneven mixing, and severe PM emissions problems Mohr *et al.* (2000). Therefore, the main problem is reducing the PM emissions in parallel with improving the thermal efficiency of GDI engines. Zong *et al.* (2004); Piock *et al.* (2011).

Given the low thermal efficiency of GDI engines and particulate problems, a method to achieve a high temperature and pressure environment in the combustion chamber during engine operation is called the fuel's supercritical environment Mayer *et al.* (2000). A fluid or a mixture of fuels is defined as being in the supercritical state if the pressure and temperature exceed all fuel species' critical values.

Supercritical fluids (SCFs) are attractive media for chemical reactions because of their unique properties. According to Liu *et al.* (2017), supercritical fluids exhibit lower viscosities and surface tension than liquids; at the same time, supercritical fluids also present high diffusion rates. Because of those properties, the uniform mixture distribution of fuel and air can effectively improve thermal efficiency and reduce the particulate emissions of the engine when supercritical fuel is injected into a cylinder in a supercritical environment (Song *et al.*, 2020).

Another way to control emissions is to use biofuels in the mixture. In this way, Lee *et al.* (2009) and Szybist *et al.*

(2011) investigated the beneficial use of ethanol as an alternative fuel to control particulate emissions from GDIs, mainly when used in high concentrations. The main finding of their study is that the use of E85 results in 1-2 orders of magnitude reduction in particle emissions relative to GDI fueling with gasoline and E20.

With that in mind, there are many reasons why someone might want to look into the combustion of ethanol. For one, there is a growing need for alternative fuel sources that are renewable and sustainable Heufer *et al.* (2012). Additionally, there is a push to reduce carbon emissions and other pollutants from traditional energy and power sources (hydrocarbon fuels). Finally, there is a need for additives that can help control engine knock Konnov (2009). These needs are rooted in a desire to be more economically and environmentally conscious.

In the literature, several kinetic models provide a comprehensive description of the reaction mechanism of ethanol oxidation. Marinov's mechanism (Marinov, 1999) was one of the earliest detailed models of ethanol oxidation. More recent kinetic models, some derived from Marinov's mechanism, have been published. These models, such as those found in references (Cancino *et al.*, 2010), Lee *et al.* (2012), (Konnov, 2009; Konnov *et al.*, 2011), (Cai and Pitsch, 2015), and (Roy and Askari, 2020), have significantly improved the description of ethanol combustion chemistry. Our study focuses on only a few available kinetic models in the literature. However, as they interest us, we will briefly discuss two recent ones in references (Cancino *et al.*, 2010) and Heufer *et al.* (2012).

According to the research paper by Cancino *et al.* (2010), their kinetic model involves 136 species and 1349 elementary reactions. They combined the mechanisms from Marinov (1999) and the C3 hydrocarbon model from Konnov (2009) to form their model. Additionally, the model incorporates up-to-date rate data for ethanol consumption reactions. It is worth noting that the Cancino *et al.* model exhibits remarkable conformity with high-pressure shock tube data (10, 30, and 50 bar) for stoichiometric and lean ethanol-air mixtures, which is particularly interesting as an initial start to analyze Ultra-High pressure combustion (supercritical combustion).

Also came an interesting research article by Heufer *et al.* (2012) on the Kinetic Modeling of n-Pentanol Oxidation. The author developed a detailed model of 599 species and 3248 reactions, validated against ignition delay times, speciation data, and laminar flame velocity measurements. The study concludes that the model agrees well with the experiments and allows for a detailed discussion of the differences between alcohols and alkanes.

Also, understanding the speed at which flames burn is essential for ensuring safe and efficient combustion. This is especially crucial when working with fuels like Ethanol (Dirrenberger *et al.*, 2014; Broustail *et al.*, 2011; Bradley *et al.*, 2009; Monteiro *et al.*, 2015) and mixtures that include Ethanol. Researchers have conducted several studies to measure these fuels and mixtures' Laminar flame speed (LFS) using flame front imaging and pressure rise measurements. Some of these studies have focused on pure Ethanol, while others have looked at mixtures with Methane, biogas (Hinton *et al.*, 2018), or n-butanol (Alviso *et al.*, 2022). By analyzing the parameters of flame speed, researchers can better understand how different fuels and blends will burn and optimize combustion for safety and efficiency.

In contrast, knowing fuel's ignition and combustion process at supercritical conditions requires a detailed study of chemical kinetics and its properties in this condition. Beyond that, simulation and analysis of high-pressure combustion, where significant species experience transcritical and supercritical states, must incorporate non-idealities in thermodynamic and chemical kinetic properties. Critical properties, such as critical temperature and pressure, are shown in Table 1 for the alcohol fuel (Ethanol), oxygen, and nitrogen.

Table 1: Critical properties of selected alcohol fuel, oxygen, and nitrogen (Poling *et al.*, 2001)

Formula	Name	Tc [K]	Pc [bar]
$C_2H_6O$ ( $C_2H_5OH$ )	ethanol	513.9	61.48
$O_2$	oxygen	154.6	50.43
$N_2$	nitrogen	126.2	33.98

Experimental ignition delay studies must be improved to validate the kinetic models used in high-pressure combustion simulations. In most cases, the kinetic treatments of high-pressure reacting mixtures assume ideal gas behavior. In this way, Kogekar *et al.* (2018) studied the real gas effects (i.e., a multi-component R-K formulation) on high-pressure combustion by comparing simulated and experimentally measured ignition delay time (IDT) from shock tube for n-dodecane/ $O_2$ / $N_2$  mixtures, using a chemical mechanism with 100 species and 432 reactions, developed by Wang *et al.* (2014). Their results demonstrate that non-ideal behavior can affect predicted IDTs by as much as 50–100  $\mu$ s in the NTC region.

The present paper focuses on a new reduced mechanism that contains ethanol (oxygenated hydrocarbon) for calculating the oxidation of supercritical ethanol. The final ethanol kinetic mechanism comprised 71 species and 684 reactions. The simulation used a 0D constant-volume auto-ignition delay times IDT, calculated by Cantera version 2.5.1 (Goodwin *et al.*, 2021). The validation was done using available experimental results under supercritical conditions of ignition delay times (IDT) at shock tube (ST) under stoichiometric equivalence ratios ( $\phi$ ), high-pressure range (10-75 atm), and temperatures between 700-1200 K. And Laminar flame speed (LFS) at 1 - 4 atm and 380 - 450 K using the ideal EoS. All the IDT simulations used the cubic Redlich-Kwong (RK) and the ideal (I) equation of states (EoS). The critical properties

of each species in the merged mechanism necessary to obtain the parameters using the cubic R-K equation of state were obtained by applying Joback's Group Method Poling *et al.* (2001); Thomson *et al.* (2008).

## 2. METHODOLOGY

### 2.1 Reduction process

The reduced mechanisms are developed using a mechanism reduction approach, which is the combination of the Directed relation graph with error propagation (DRGEP) (Pepiot-Desjardins and Pitsch, 2008) and the sensitivity analysis (SA) (Rabitz *et al.*, 1983; Turányi, 1990). All these features are available in Pymars code, version 1.1.0, developed by Mestas *et al.* (2019).

The present work achieved the ethanol-reduced model by reducing the Cancino *et al.* (2010) (136 species and 1349 reactions). Concerning that the Cancino *et al.* (2010) ethanol mechanism was validated using only IDT experimental results obtained in an ST at 10, 30, and 50 bar, no 1D freely propagating flames were considered in Cancino *et al.* work. So, before the reduced process, we tried to run it in Cantera using an LFS approach. But it does not run because it presents three duplicate reactions ' $C_2H_5OH + HO_2 \rightleftharpoons SC_2H_5O + H_2O_2$ ', in which one of them exhibits the largest pre-exponential factor of the mechanism that is equal to  $10^{129}$ , which struggles to reach convergence. However, when we decrease the pre-exponential factor one step by time, the simulation of LFS starts to run when the pre-exponential factor equals  $10^{100}$ . Besides, the resulting original mechanism with the highest pre-exponential factor  $10^{100}$  is referred to as the "Original mechanism" (Original M.). The true original ethanol Cancino *et al.* (2010) mechanism with the highest pre-exponential factor  $10^{129}$  is referred as "Original\* mechanism" (Original\* M.).

The ethanol model reduction was performed based on operating conditions for 0D constant-volume IDT for two equivalence ratios, corresponding to a lean ( $\phi = 0.50$ ) and a stoichiometric mixture ( $\phi = 1.0$ ), and the temperature range of  $700 \leq T \leq 1280$  K at pressures of about 10, 30, 50 and 70 atm. The interactive removal of reactions and species in the DRGEP reduction occurs until a defined threshold of 1% error in IDT, computed overall conditions of interest. DRGEP targets included species OH, CO, and the hydroperoxy radical ( $HO_2$ ), acetaldehyde ( $CH_3HCO = C_2H_4O$ ), hydrogen peroxide ( $H_2O_2$ ), and 1-hydroxyethyl radical  $CH_3CHOH$  (named "SC2H5O" in Cancino *et al.* (2010)) to the Ethanol reduction process due to their highest sensitivity pressure. In the reduction process, the target combustion products were  $CO_2$  and  $H_2O$ . After all these processes, the reduced kinetic model of Ethanol consists of 71 species and 684 reactions.

All the mechanisms used in the reduced process are summarized in Tab. 2.

Table 2: Ethanol mechanisms

Name	Species	Reaction	Type	Reference
Ethanol OM	136	1349	Detailed	Cancino <i>et al.</i> (2010)
Ethanol RM	71	684	Reduced	-

OM, Original mechanism; RM, Reduced mechanism;

### 2.2 Real Equations of state: properties

Although the ideal (I) equation of states (EoS) was used until here, to understand better the magnitude of the real gas effects on reflected shock tube IDTs at high-pressure combustion, it is necessary consideration of an accurate gas equation of state at the simulations. This goal is supported using the cubic multi-component Redlich-Kwong equation of state in CANTERA Goodwin *et al.* (2021). This R-K EoS implementation gives qualitatively accurate results across a range of non-ideal states, and its accuracy suffers in the liquid-vapor equilibrium region. The present study uses a multi-component, mixture-averaged form of the R-K EoS to predict real gas behavior.

For a pure species, The R-K EoS is:

$$P = \frac{RT}{V - b} - \frac{a}{T^{1/2}V(V + b)}; \quad (1)$$

$$a = 0.42748 \frac{R^2 T_c^{5/2}}{P_c}; \quad (2)$$

$$b = 0.08664 \frac{RT_c}{P_c} \quad (3)$$

Here, the influence of molecular interactions is given by the species-specific Van der Waals attraction parameter (a) and repulsive volume correction parameter (b). Where P is the pressure (Pa); V is the molar volume ( $m^3 mol^{-1}$ ); R is



### 3. RESULTS AND DISCUSSIONS

As discussed in subsection 2.1, the Ethanol original\* mechanism of Cancino *et al.* (2010) presents the highest pre-exponential factor  $10^{129}$  in duplicate reaction ' $C_2H_5OH + HO_2 \rightleftharpoons SC_2H_5O + H_2O_2$ ', resulting in a minor IDT at intermediate-lower temperatures when compared with the "Ethanol Original mechanism" with the highest pre-exponential factor  $10^{100}$ . However, no 1D freely propagating flames were considered in Cancino *et al.* work.

As a comparison between the Ethanol reduced M. and the Ethanol original M. ( $100^{100}$ ), a laminar flame speed (LFS) run was performed in Cantera using an initial temperature of 380 K, Pressure equal to 2 atm, and equivalence ratios range ( $\phi = 0.7$  to 1.4), as demonstrated in Fig. 2(a). This LFS simulation exhibits an excellent agreement between the reduced and the original ethanol mechanism. However, it presents a considerable deviation from the experimental data of Hinton *et al.* (2018), mainly in lean and stoichiometric equivalence ratios.

A laminar flame speed(LFS) sensitivity was performed to improve the Ethanol reduced mechanism LFS simulations regarding the conditions of the Hinton *et al.* (2018) experimental data, and a straightforward approach consisted of modifying the most critical reactions pre-exponential factor (A) of Arrhenius equation at the target conditions, as performed for IDT in the study of Song *et al.* (2019) for a gasoline surrogate mixture mechanism.

Figure. 2(b) shows LFS simulation at the same operating conditions of Hinton *et al.* (2018), but after modifying the pre-exponential factor of some main reactions. It is possible to notice better accordance between the Ethanol reduced M. and the LFS experimental data at all ranges of equivalence ratios.

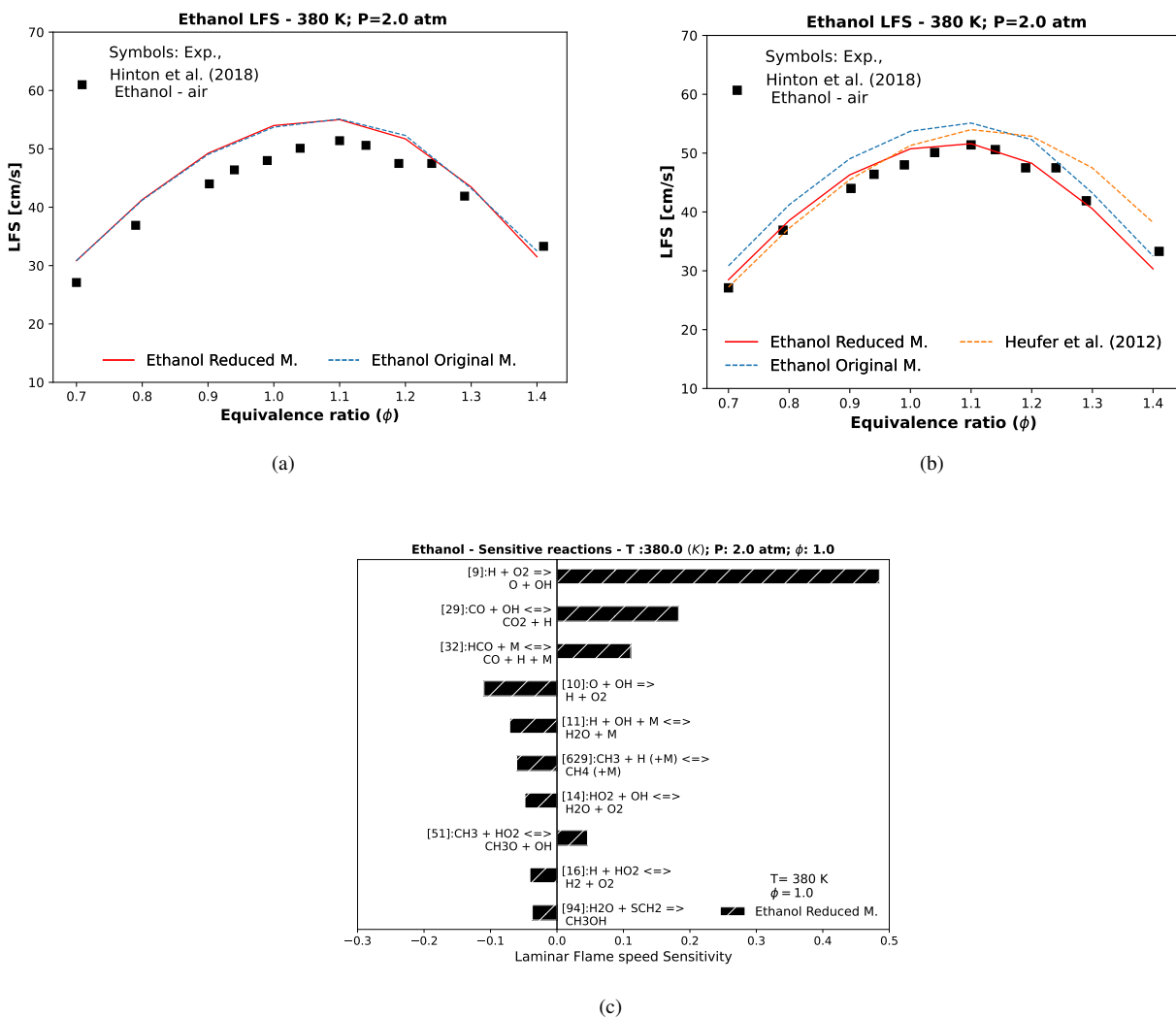


Figure 2: Numerical stoichiometric LFS simulation at different pressure considering the Ethanol reduced mechanism versus (a) the original mechanism with the highest pre-exponential factor  $10^{100}$  before modifying the pre-exponential factor (A) of main reactions, and (b) after modifying (A) use ideal EoS, c) represents the Laminar flame speed sensitivity to select the main reactions at target conditions.

Concerning the modifying pre-exponential factor approach, Figure. 2(c) shows the ten most sensitive reactions from the Hinton *et al.* experimental selected conditions for Stoichiometric Ethanol laminar flame speed.

All the modifications of the pre-exponential factor of the first three reactions numbered [9], [29], [32] are according to the previous Hydrogen, and Ethanol literature from GALWAY Database (Zhang *et al.*, 2017; Heufer *et al.*, 2012; Mittal *et al.*, 2014; Zhang *et al.*, 2018). Furthermore, the mechanism from Heufer *et al.* (2012) is a detailed Pentanol mechanism containing Ethanol (EM) and presents 599 species and 3248 reactions, which is much more species and reactions than the ethanol-reduced mechanism with 71 species and 684 reactions presented here.

Table 3: Modifying the pre-exponential factor of Ethanol

Reaction	Previous (A)	Modified (A)	Reference (GALWAY Database)
R. [9] $\text{H} + \text{O}_2 \Rightarrow \text{O} + \text{OH}$	9.75e+13	1.04e+14	Zhang <i>et al.</i> (2017), Zhang <i>et al.</i> (2018)
R. [29] $\text{CO} + \text{OH} \Leftrightarrow \text{CO}_2 + \text{H}$	1.17e+07	5.76e+12	Heufer <i>et al.</i> (2012), Zhang <i>et al.</i> (2018)
Duplicate Reaction	-	7.01e+04	Zhang <i>et al.</i> (2018), Mittal <i>et al.</i> (2014)
R. [32] $\text{HCO} + \text{M} \Leftrightarrow \text{CO} + \text{H} + \text{M}$	1.56e+14	5.70E+11	Zhang <i>et al.</i> (2018), Mittal <i>et al.</i> (2014)
R. [16] $\text{H} + \text{HO}_2 \Leftrightarrow \text{H}_2 + \text{O}_2$	4.28e+13	1.140e+10	Zhang <i>et al.</i> (2017), Mittal <i>et al.</i> (2014)

After all this process with LFS, and as described in the methodology section, the IDT simulations of the mixture Ethanol/air as a function of temperature for stoichiometric combustion conditions ( $\phi = 1$ ), pressures of 1, 10, 50, and 100 atm, and initial temperatures in the range between 700 and 1250 K are presented in Fig. 3(a). Besides, the resulting original mechanism with the highest pre-exponential factor  $10^{100}$  (Original M.) at higher-intermediate temperature conditions agrees well with The genuine original ethanol Cancino *et al.* (2010) mechanism with the highest pre-exponential factor  $10^{129}$  ("Original\* M.) although present a higher deviation at lower intermediate temperature conditions.

Figure 3(b) shows that the Ethanol reduced mechanism agrees well with its Ethanol original mechanism in all the selected conditions (1, 10, 50, and 100 atm) and the highest difference of IDT simulation results between reduced mechanisms and the original Ethanol were 1.0%.

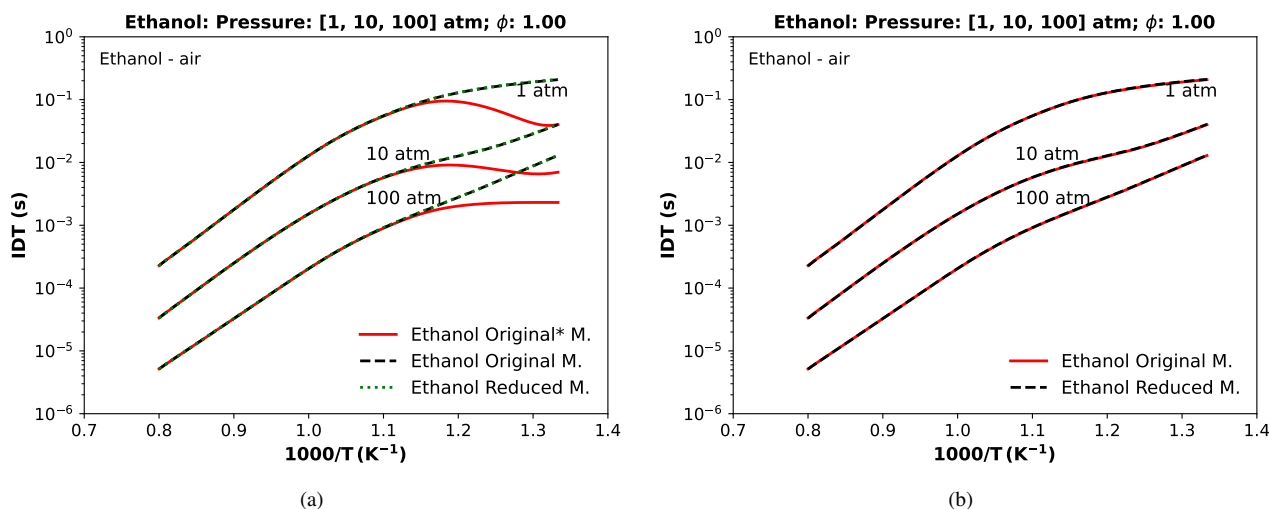


Figure 3: Numerical stoichiometric IDT at different pressure considering the Ethanol reduced mechanism against (a) the original mechanism with the highest pre-exponential factor  $10^{100}$ , versus the Ethanol original\* mechanism of Cancino *et al.* (2010) with the highest pre-exponential  $10^{129}$  (1, 10, 100 atm) and (b) versus the first one. Both simulations use ideal EoS.

### 3.1 Ethanol IDT

After the reduction, various experimental conditions of shock tube (ST) data are collected to compare the Ethanol-reduced mechanism at more comprehensive pressure and temperature conditions. Shock tube (ST) data for Ethanol from (Cancino *et al.*, 2009; Heufer and Olivier, 2010; Heufer *et al.*, 2011; Zyada and Samimi-Abianeh, 2019).

Figure 4(a) shows the reasonable agreement of the ethanol-reduced mechanism with the experimental ethanol data of ignition delay time (IDT) at different pressures using a sub-critical shock tube at 20 atm and a supercritical shock tube (ST) at 75 atm pressure (Heufer and Olivier, 2010). Also, Figure 4(b) shows a sub-critical experimental data at 13 and 40 atm pressure (Heufer *et al.*, 2011; Zyada and Samimi-Abianeh, 2019).

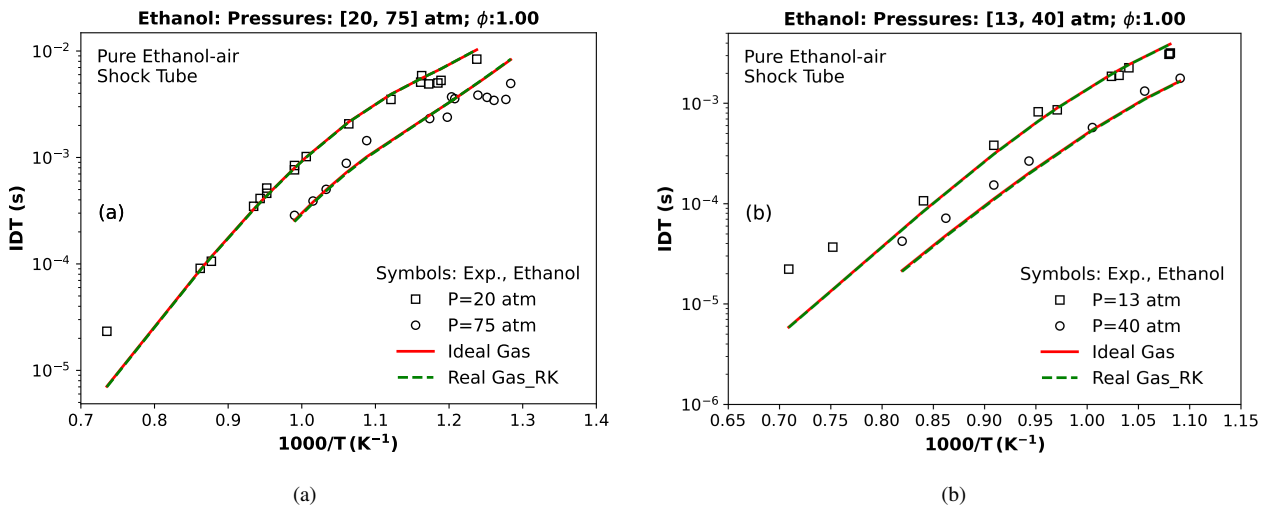


Figure 4: IDT simulations against (a) a sub-critical shock tube (ST) data at 20 atm and a supercritical (ST) data at 75 atm (Heufer *et al.*, 2011); and (b) a sub-critical data at 13, and at 40 atm (Heufer *et al.*, 2011; Zyada and Samimi-Abianeh, 2019) using a stoichiometric mixture composition of Ethanol,  $O_2$ , and  $N_2$ ; Symbols represent experiments; solid and dashed lines are the Ethanol reduced mechanism, respectively, using the ideal (I) and the real gas Redlich-Kwong (RK) EoS.

Figure 5(a) shows the numerical IDT of ethanol/air against the experimental data from Cancino *et al.* (2010), respectively, at 10 (sub-critical) and 50 atm (supercritical). At 10 atm pressure conditions, a relatively large deviation is observed at intermediate-lower temperatures for this ethanol-reduced mechanism, whereas improved agreement can be observed at intermediate-higher temperatures.

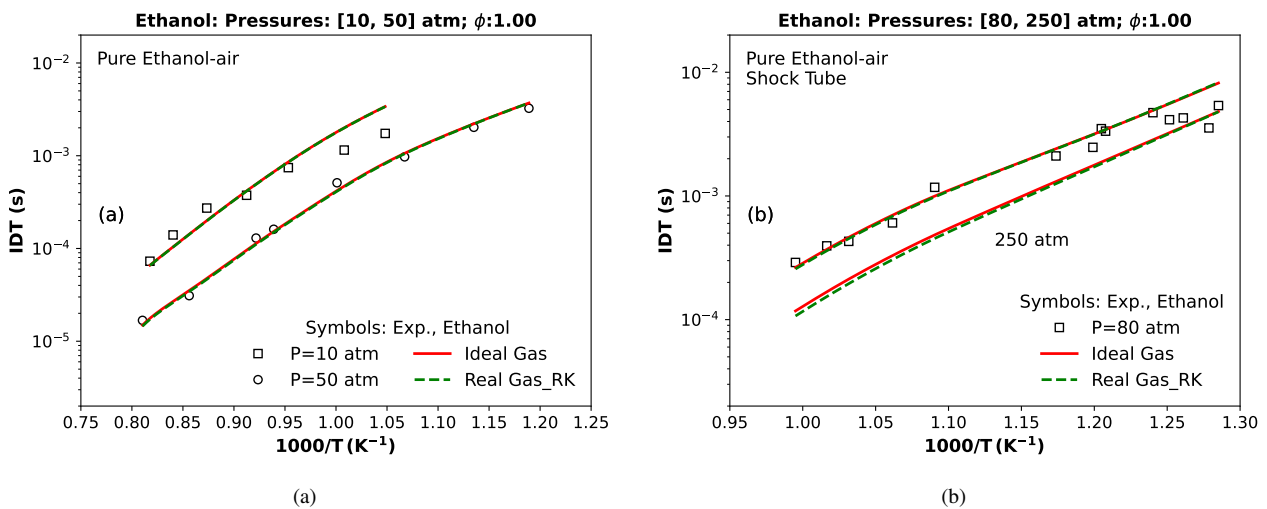


Figure 5: IDT simulations against (a) a sub-critical shock tube (ST) data at 10 and 50 atm (Cancino *et al.*, 2010); and (b) a supercritical shock tube (ST) data at 80 (Lee *et al.*, 2012), and also a supercritical simulation at 250 atm using a stoichiometric mixture composition of Ethanol,  $O_2$ , and  $N_2$ ; Symbols represent experiments; solid and dashed lines are the Ethanol reduced mechanism, respectively, using the ideal (I) and the real gas Redlich-Kwong (RK) EoS.

In Figure 5(b), the same pure Ethanol/air mixture is validated against supercritical shock tube experimental data of Lee *et al.* (2012) at 80 atm; Also, in Figure 5(b) is possible to notice an increase in pressure (80 to 250 atm) promotes 9% the deviation between simulations using the ideal gas (I) and real gas (RK) equation of states.

### 3.2 Ethanol LFS

To validate the mechanism for a broader range, different temperature and pressure conditions are considered in sub-critical conditions. No Laminar flame speed (LFS) experimental data is available at supercritical conditions in the literature.

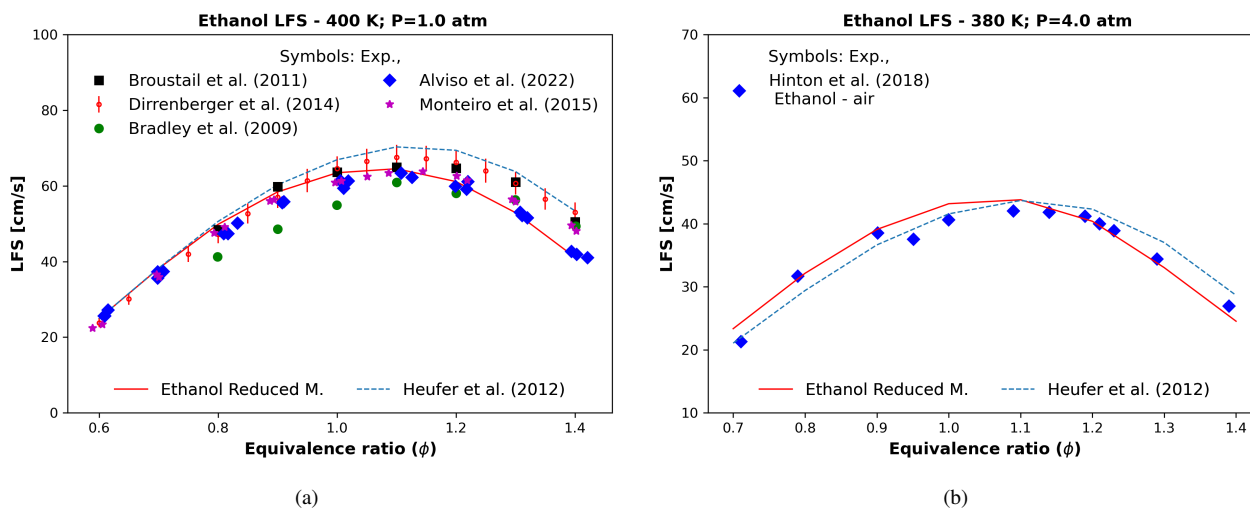


Figure 6: Ethanol LFS reduced model results compared to the LFS experimental data of a) Broustail *et al.* (2011), Dirrenberger *et al.* (2014), Bradley *et al.* (2009), Alviso *et al.* (2022), and Monteiro *et al.* (2015) at 400 K and 1 atm, b) Hinton *et al.* (2018) at 380 K and 4 atm. Dotted lines are the literature mechanism (Heufer *et al.*, 2012). All FLS simulations using the ideal (I) EoS.

The results at atmospheric pressure and 400 K, in Fig. 6(a), are in excellent agreement with most of the recent experimental data found in literature (Alviso *et al.*, 2022), which shows the resulting Ethanol-reduced mechanism gives reliable results at atmospheric pressure. Beyond that, it is found that the Ethanol reduced model agrees well with the experiment at 380 K and 4 atm conditions, as shown in Fig. 6(b) for 1D Laminar flame speed simulations. Based on Figures 6(a) and 6(b), the Ethanol Reduced M. gives reliable results even when compared with more extensive detailed literature kinetic models, which is the case of (Heufer *et al.*, 2012) comprising 599 species and more than 3000 reactions.

### 4. CONCLUSIONS

This work obtained a reduced model for simulating supercritical Ethanol; the model comprises 71 species and 684 reactions.

This new mechanism was validated using sub-critical and supercritical experimental data of ignition delay times (IDT) for pure ethanol as a function of temperature and pressure. Under the operating conditions studied here, incorporating non-idealities decreases the predicted ignition times by approximately 3% between R–K and ideal gas EoS simulations at 80 atm. Although the non-ideal effects are moderate at 75 atm, they increase in significance at elevated operating pressures. At 250 atm, the relative difference between ideal and real gas EoS predicted ignition delay times is roughly 9% in higher temperature regions for Ethanol.

Based on the available experimental data for ethanol combustion, the Ethanol reduced mechanism does a pretty good job of reproducing the results of IDT at both sub-critical and supercritical conditions. Although there are some discrepancies between the model's predictions and the actual experimental results, the subcritical predictions for the flame species are reasonably accurate, especially when considering the uncertainties that arise from changes in the pre-exponential factor. Overall, this mechanism performs well across various temperature and pressure conditions.

### 5. ACKNOWLEDGEMENTS

The support of Fundação de Desenvolvimento da Pesquisa – Fundep, Rota 2030 - Linha V to the first author in the form of a Ph.D. Program Scholarship is gratefully acknowledged.

### 6. REFERENCES

Alviso, D., Garcia, A., Mendieta, M., Gonçalves dos Santos, R. and Darabiha, N., 2022. "Experimental and kinetic modeling studies of laminar flame speed of n-butanol/ethanol blends". *Journal of the Brazilian Society of Mechanical*

*Sciences and Engineering*, Vol. 44, No. 6, p. 222.

- Binder, A., Ecker, R., Glaser, A. and Müller, K., 2015. "Gasoline direct injection". In *Gasoline Engine Management*, Springer, pp. 110–121.
- Bradley, D., Lawes, M. and Mansour, M., 2009. "Explosion bomb measurements of ethanol–air laminar gaseous flame characteristics at pressures up to 1.4 mpa". *Combustion and Flame*, Vol. 156, No. 7, pp. 1462–1470.
- Broustail, G., Seers, P., Halter, F., Moréac, G. and Mounaïm-Rousselle, C., 2011. "Experimental determination of laminar burning velocity for butanol and ethanol iso-octane blends". *Fuel*, Vol. 90, No. 1, pp. 1–6.
- Cai, L. and Pitsch, H., 2015. "Optimized chemical mechanism for combustion of gasoline surrogate fuels". *Combustion and flame*, Vol. 162, No. 5, pp. 1623–1637.
- Cancino, L., Fikri, M., Oliveira, A. and Schulz, C., 2009. "Autoignition of gasoline surrogate mixtures at intermediate temperatures and high pressures: Experimental and numerical approaches". *Proceedings of the Combustion Institute*, Vol. 32, No. 1, pp. 501–508.
- Cancino, L., Fikri, M., Oliveira, A. and Schulz, C., 2010. "Measurement and chemical kinetics modeling of shock-induced ignition of ethanol- air mixtures". *Energy & Fuels*, Vol. 24, No. 5, pp. 2830–2840.
- Dirrenberger, P., Glaude, P.A., Bounaceur, R., Le Gall, H., Da Cruz, A.P., Konnov, A. and Battin-Leclerc, F., 2014. "Laminar burning velocity of gasolines with addition of ethanol". *Fuel*, Vol. 115, pp. 162–169.
- Goodwin, D.G., Speth, R.L., Moffat, H.K. and Weber, B.W., 2021. "Cantera: An object-oriented software toolkit for chemical kinetics, thermodynamics, and transport processes". <https://www.cantera.org>. doi: 10.5281/zenodo.4527812. Version 2.5.1.
- Heufer, K.A., Sarathy, S.M., Curran, H.J., Davis, A.C., Westbrook, C.K. and Pitz, W.J., 2012. "Detailed kinetic modeling study of n-pentanol oxidation". *Energy & Fuels*, Vol. 26, No. 11, pp. 6678–6685.
- Heufer, K. and Olivier, H., 2010. "Determination of ignition delay times of different hydrocarbons in a new high pressure shock tube". *Shock Waves*, Vol. 20, No. 4, pp. 307–316.
- Heufer, K., Uygun, Y., Olivier, H., Vranckx, S., Lee, C. and Fernandes, R., 2011. "Experimental study of the high-pressure ignition of alcohol based biofuels". In *Proc. European Combust Meeting*.
- Hinton, N., Stone, R. and Cracknell, R., 2018. "Laminar burning velocity measurements in constant volume vessels– reconciliation of flame front imaging and pressure rise methods". *Fuel*, Vol. 211, pp. 446–457.
- Joback, K.G., 1984. *A unified approach to physical property estimation using multivariate statistical techniques*. Ph.D. thesis, Massachusetts Institute of Technology.
- Kogekar, G., Karakaya, C., Liskovich, G.J., Oehlschlaeger, M.A., DeCaluwe, S.C. and Kee, R.J., 2018. "Impact of non-ideal behavior on ignition delay and chemical kinetics in high-pressure shock tube reactors". *Combustion and Flame*, Vol. 189, pp. 1–11.
- Konnov, A., 2009. "Implementation of the ncn pathway of prompt-no formation in the detailed reaction mechanism". *Combustion and Flame*, Vol. 156, No. 11, pp. 2093–2105.
- Konnov, A., Meuwissen, R. and De Goey, L., 2011. "The temperature dependence of the laminar burning velocity of ethanol flames". *Proceedings of the Combustion Institute*, Vol. 33, No. 1, pp. 1011–1019.
- Lee, C., Vranckx, S., Heufer, K.A., Khomik, S.V., Uygun, Y., Olivier, H. and Fernandez, R.X., 2012. "On the chemical kinetics of ethanol oxidation: shock tube, rapid compression machine and detailed modeling study". *Zeitschrift für Physikalische Chemie*, Vol. 226, No. 1, pp. 1–28.
- Lee, J., Patel, R., Schonborn, A., Ladommatos, N. and Bae, C., 2009. "Effect of biofuels on nanoparticle emissions from spark-and compression-ignited single-cylinder engines with same exhaust displacement volume". *Energy & fuels*, Vol. 23, No. 9, pp. 4363–4369.
- Li, S., Williams, G. and Guo, Y., 2016. "Health benefits from improved outdoor air quality and intervention in china". *Environmental Pollution*, Vol. 214, pp. 17–25. ISSN 0269-7491. doi:<https://doi.org/10.1016/j.envpol.2016.03.066>. URL <https://www.sciencedirect.com/science/article/pii/S0269749116302470>.
- Liu, Y., Pei, Y., Peng, Z., Qin, J., Zhang, Y., Ren, Y. and Zhang, M., 2017. "Spray development and droplet characteristics of high temperature single-hole gasoline spray". *Fuel*, Vol. 191, pp. 97–105.
- Marinov, N.M., 1999. "A detailed chemical kinetic model for high temperature ethanol oxidation". *International Journal of Chemical Kinetics*, Vol. 31, No. 3, pp. 183–220.
- Mayer, W., Schik, A., Schaffer, M. and Tamura, H., 2000. "Injection and mixing processes in high-pressure liquid oxygen/gaseous hydrogen rocket combustors". *Journal of Propulsion and Power*, Vol. 16, No. 5, pp. 823–828.
- Mestas, P., Clayton, P. and Niemeyer, K., 2019. "pymars: automatically reducing chemical kinetic models in python". *Journal of Open Source Software*, Vol. 4, No. 41.
- Mittal, G., Burke, S.M., Davies, V.A., Parajuli, B., Metcalfe, W.K. and Curran, H.J., 2014. "Autoignition of ethanol in a rapid compression machine". *Combustion and Flame*, Vol. 161, No. 5, pp. 1164–1171.
- Mohr, M., Steffen, D. and Forss, A.M., 2000. *Particulate emissions of gasoline vehicles and influence of the sampling procedure*. SAE International.
- Monteiro, J.O.D. et al., 2015. "Laminar flame speed of fuel mixtures applied to spark ignition internal combustion

engines”.

- Owczarek, I. and Blazej, K., 2003. “Recommended critical temperatures. part i. aliphatic hydrocarbons”. *Journal of Physical and Chemical Reference Data*, Vol. 32, No. 4, pp. 1411–1427.
- Owczarek, I. and Blazej, K., 2004. “Recommended critical temperatures. part ii. aromatic and cyclic hydrocarbons”. *Journal of physical and chemical reference data*, Vol. 33, No. 2, pp. 541–548.
- Pepiot-Desjardins, P. and Pitsch, H., 2008. “An efficient error-propagation-based reduction method for large chemical kinetic mechanisms”. *Combustion and Flame*, Vol. 154, No. 1-2, pp. 67–81.
- Piock, W., Hoffmann, G., Berndorfer, A., Salemi, P. and Fusshoeller, B., 2011. “Strategies towards meeting future particulate matter emission requirements in homogeneous gasoline direct injection engines”. *SAE International Journal of Engines*, Vol. 4, No. 1, pp. 1455–1468.
- Poling, B., Prausnitz, J. and O’Connell, J., 2001. *The Properties of Gases and Liquids*. McGraw-Hill, 5<sup>th</sup> edition.
- Rabitz, H., Kramer, M. and Dacol, D., 1983. “Sensitivity analysis in chemical kinetics”. *Annual review of physical chemistry*, Vol. 34, No. 1, pp. 419–461.
- Roy, S. and Askari, O., 2020. “A new detailed ethanol kinetic mechanism at engine-relevant conditions”. *Energy & Fuels*, Vol. 34, No. 3, pp. 3691–3708.
- Song, Y., Zheng, Z., Peng, T., Yang, Z., Xiong, W. and Pei, Y., 2020. “Numerical investigation of the combustion characteristics of an internal combustion engine with subcritical and supercritical fuel”. *Applied Sciences*, Vol. 10, No. 3, p. 862.
- Song, Y., Zheng, Z. and Xiao, J., 2019. “Development and validation of a reduced chemical kinetic mechanism for supercritical gasoline of gdi engine”. *Fuel*, Vol. 241, pp. 676–685.
- Szybist, J.P., Youngquist, A.D., Barone, T.L., Storey, J.M., Moore, W.R., Foster, M. and Confer, K., 2011. “Ethanol blends and engine operating strategy effects on light-duty spark-ignition engine particle emissions”. *Energy & Fuels*, Vol. 25, No. 11, pp. 4977–4985.
- Thomson, G.H., Friend, D.G., Rowley, R.L., Wilding, W.V. and Poling, B.E., 2008. “Physical and chemical data section 2”. *Perry’s chemical engineer’s handbook*. McGraw-Hill, New york, pp. 2–48.
- Turányi, T., 1990. “Sensitivity analysis of complex kinetic systems. tools and applications”. *Journal of mathematical chemistry*, Vol. 5, No. 3, pp. 203–248.
- Wang, H., Ra, Y., Jia, M. and Reitz, R.D., 2014. “Development of a reduced n-dodecane-pah mechanism and its application for n-dodecane soot predictions”. *Fuel*, Vol. 136, pp. 25–36.
- Zhang, Y., El-Merhubi, H., Lefort, B., Le Moyne, L., Curran, H.J. and Keromnes, A., 2018. “Probing the low-temperature chemistry of ethanol via the addition of dimethyl ether”. *Combustion and Flame*, Vol. 190, pp. 74–86.
- Zhang, Y., Mathieu, O., Petersen, E.L., Bourque, G. and Curran, H.J., 2017. “Assessing the predictions of a nox kinetic mechanism on recent hydrogen and syngas experimental data”. *Combustion and Flame*, Vol. 182, pp. 122–141.
- Zong, N., Meng, H., Hsieh, S.Y. and Yang, V., 2004. “A numerical study of cryogenic fluid injection and mixing under supercritical conditions”. *Physics of fluids*, Vol. 16, No. 12, pp. 4248–4261.
- Zyada, A. and Samimi-Abianeh, O., 2019. “Ethanol kinetic model development and validation at wide ranges of mixture temperatures, pressures, and equivalence ratios”. *Energy & Fuels*, Vol. 33, No. 8, pp. 7791–7804.

## 7. RESPONSIBILITY NOTICE

The authors are solely responsible for the printed material included in this paper.